Some Specific Challenges of HLFC Design on a Long-range Wing

Geza Schrauf[1] and Thomas Kilian[2]

[1] Retired from DLR, 38108 Braunschweig, Germany,
contact@schrauf.de,
[2] DLR, 38108 Braunschweig, Germany,
thomas.kilian@dlr.de

Abstract. We describe the aerodynamic design of an HLFC system for the wing of a large transport aircraft and compare it to the the HLFC system installed in the VTP of the DLR A320 ATRA aircraft. For the VTP we used the ALTTA-design with a laser-drilled microperforated titanium sheet with only one microperforation and small suction chambers beneath it. For the wing we designed a system with only one large plenum and controlled the suction with the help of variable microperforation. Some specific challenges of an HLFC design on a wing in contrast to a VTP application are highlighted here.

Keywords: Hybrid Laminar Flow Control (HLFC), suction system design, variable microperforation, A320 VTP, HLFC wing

1 Introduction to the HLFC-WIN project

The European project HLFC-WIN is developing a hybrid-laminar-flow-control (HLFC) system for the wing of a long-range aircraft as part of Clean Sky 2. The configuration considered for the project is shown in Figure 1. The wing is based on the turbulent XRF1 research configuration provided by Airbus.

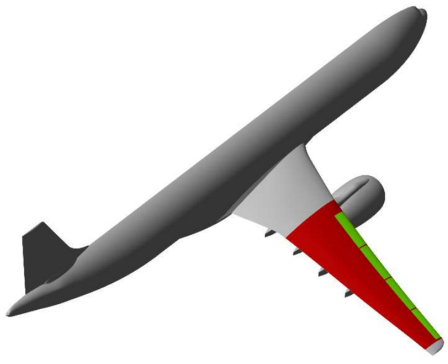

Fig. 1: Configuration for HLFC-WIN project.

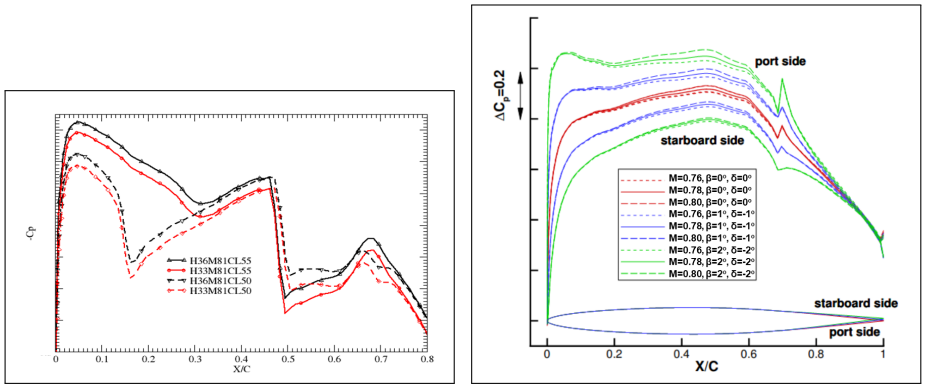

(a) HLFC wing. (b) A320 VTP.

Fig. 2: Comparison of two pressure distributions.

Fig. 3: The A320 aircraft with the HLFC system installed in the VTP.

For the purpose of this project, the wing planform was not altered, only the airfoil sections outboard of the engine (cf. red area in Figure 1) were changed to favor HLFC [1].

The wing pressure distribution has a suction peak followed by a pressure recovery as shown in Figure 2a. This differs from the pressure distribution considered for earlier HLFC applications, as, for example, in that of the A320 VTP presented in Figure 2b. The design of the HLFC system for the VTP and some flight test results are described in [2, 3]. The installed VTP system is shown in Figure 3.

The pressure distribution of the HLFC wing also differs from that of the HLFC wing designed in the nineties within the ELFIN II project. This system was built and successfully tested in the ONERA S1MA wind tunnel [4].

For the HLFC-WIN project, we used the design idea of a pressure recovery over the suction panel (ending at $x/c = 0.29$) to allow for a region of decreasing pressure, i.e. with an accelerated boundary layer, behind the panel and before the shock. This enables a delay of the Tollmien-Schlichting (TS) transition without lowering the pressure level before the shock. The shock strength, and with that,

the wave drag, is therefore not increased. The disadvantage of this pressure distribution is the need for stronger suction, not only to suppress, as usual, cross-flow (CF) transition, but also to avoid TS-transition and, possibly, laminar separation in the pressure recovery region. The size of this region varies strongly throughout the flight envelope. For some cases it even extends beyond the front spar location which usually limits the suction area.
We have 27 design cases for the HLFC wing shown in Table 2. The cases in which the pressure distributions differ most are shown in Figure 2a. Other important differences between the current HLFC wing and the A320 VTP are the higher Mach number and the lower leading-edge sweep. A comparison of these two design parameters is given in the following table:

	Wing	VTP
Mach number	0.83 ± 0.02	0.78 ± 0.02
Leading edge sweep	33^o	40^o

Table 1: Mach numbers and sweep angles for wing and VTP.

For the wing we consider a higher Mach number in combination with a smaller sweep angle, and a larger radius of curvature. Thus we need to apply stronger suction at the leading edge to keep the attachment line laminar.

2 HLFC design requirements

Within HLFC design we control the laminar-turbulent transition with the help of boundary layer suction. At the same time, we have to make sure that no early transition is provoked by local reverse flow or by other detrimental effects such as "over-suction," i.e. equivalent roughness[1].

The general requirements for any HLFC design are listed here:

R1 Keep the attachment line laminar, i.e. satisfy the K-criterion [5, 6].
R2 Apply enough suction where boundary layer is close to laminar separation.
R3 Apply enough suction to suppress CF- and delay TS-transition.
R4 Avoid outflow.
R5 Allow for local blockage caused by supporting structural elements, such as stringers.
R6 Avoid transition by equivalent roughness: $Re_{rr} < 400 - 450$.
R7 Avoid choking in the suction holes: $M_{hole} < 0.3$.
R8 Minimize mass flow and suction power.
R9 Aim for a robust design, i.e. allow for a large variation of the microperforation and other manufacturing deviations.

[1] The flow into a suction hole forms an ending stream tube [7, Figure 1], which acts like a 3D roughness element. The height h of the roughness corresponds to the height r of the stream tube. Therefore, we can apply the criterion for a 3D roughness element shown in [8].

The requirements R1 to R5 are are strict, meaning that if one of them is violated, laminarity is lost. Requirements R7 to R9 are good design guidelines. The values given here can be relaxed.
The design of the HLFC system for the A320 VTP is described in [2]. Here we repeat only some aspects explaining the design differences between the HLFC wing and the VTP.

3 Some aspects of the design of the A320 HLFC VTP

For the VTP, the computation of the suction velocities for the aerodynamic design was based on the pressure-loss characteristic of the microperforated panel

$$\Delta p \;=\; A\,\frac{\mu_s}{\mu_0}\,w_s \;+\; B\,\frac{\rho_s}{\rho_0}\,w_s^2, \tag{1}$$

and not on any geometric quantities of the suction holes, such as hole diameter or hole pitch. To be able to proceed with the design simultaneous with the development of the laser-drilling process, we defined a range of allowable pressure-loss characteristics shown in Figure 4,

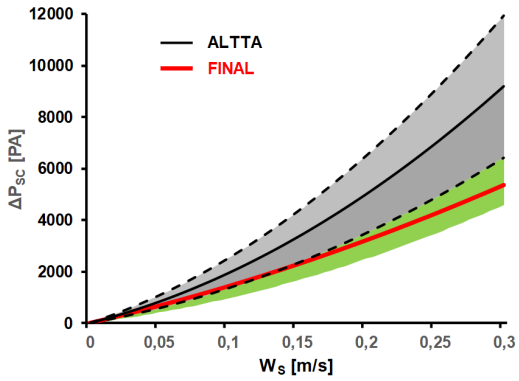

Fig. 4: Range of allowable pressure loss characteristics for the VTP design.

which is a reproduction of [2, Figure 3]. The manufacturer has to make sure that the pressure-loss characteristic of the large microperforated titanium sheet is, everywhere on the sheet, within this range. This allows for some inaccuracies occurring when producing large sheets.
In Figure 5a we present the dimensional outer pressure for the case with the largest variation of the outer pressure. The difference between the stagnation pressure and the pressure of the local minimum is 12500 Pa. It is a good design practice to work with a duct or plenum pressure p_d which is $2000-3000$ Pa below the minimum, so that the difference between outer and plenum pressure is, in the worst case, 14500 Pa. Using one microperforation, we control the suction

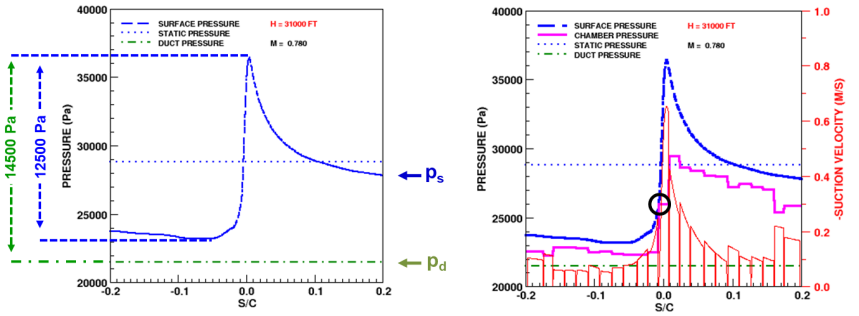

(a) Outer pressure.

(b) Chamber pressures and suction velocities.

Fig. 5: Dimensional pressures and suction velocities for 31000 ft, Mach = 0.78, side slip angle $\beta = 2^o$, rudder deflection angle $\delta = -2^o$.

velocities with the help of the chamber pressures, which are set by suitable throttle holes (cf. [2, section III.C]. The chamber pressures are shown in Figure 5b with the pink line, and the suction velocities are inserted in red with a second scale. Please note the small no-suction zones between the chambers. They are a result of the local blockage of the suction caused by the stringers. The black circle in the figure is the critical location for this case: here, the chamber pressure is only slightly lower than the outer pressure. An increase of the chamber size or of the duct pressure p_d would result in a reverse flow out of the chamber and trigger laminar-turbulent transition.

4 Some aspects of the design of the HLFC Wing

In order to limit the length of the leading edge parts, the wing outboard of the engine was divided into four segments. In this paper, we concentrate on the middle section of segment 3 at 74% span or section S74 shown in Figure 6. The design points for the HLFC wing are listed in Table 2:

Flight level	330, 360, 390
Mach number	0.81, 0.83, 0.85
Lift coefficient	0.45, 0.50, 0.55

Table 2: Design points for the HLFC wing.

The dimensional outer pressure for the case 33000 ft, Mach = 0.81, $C_L = 0.50$ is shown in Figure 7a. In this case, the difference between the stagnation pressure and the pressure in the local minimum is 20100 Pa. This high pressure difference is due to the relatively larger lift requirements of a wing compared to a VTP application and directly impacts on the system requirements. As before,

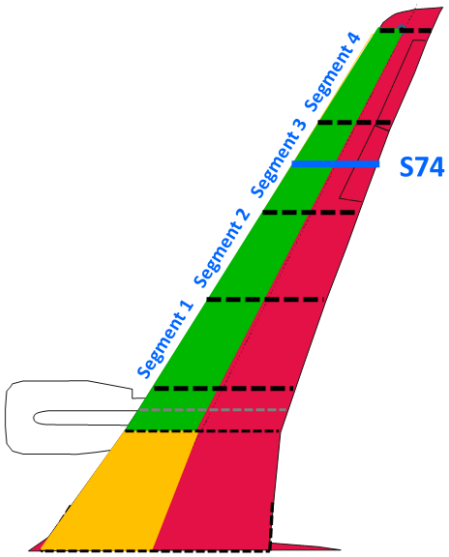

Fig. 6: Top view on wing, segment 3 with section S74.

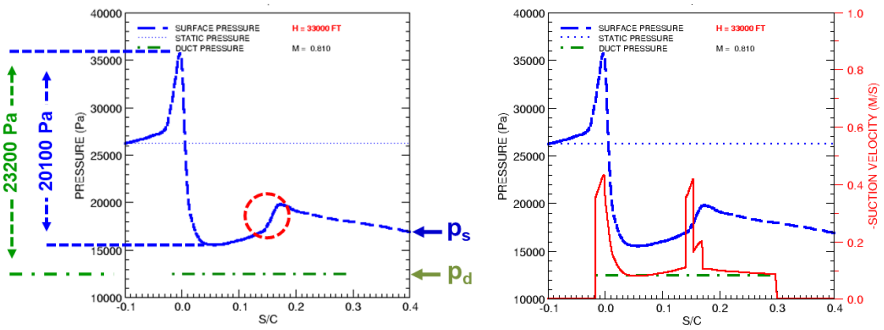

(a) Outer pressure and plenum pressure. (b) ... with suction velocity.

Fig. 7: Pressures and suction velocity for 33000 ft, Mach = 0.81, $C_L = 0.50$.

we have to consider a plenum or duct pressure P_d which is 2000 Pa lower than this minimum.

Furthermore, we notice the strong pressure recovery marked with the red circle in Figure 7a. Here, the boundary layer exhibits not only strong TS-amplification, but even worse, laminar separation. Fortunately, the separation can be avoided by applying sufficiently strong suction as shown in Figure 7b. Thus, we have to apply much stronger suction to prevent separation than would be necessary to only dampen TS-amplification. In a future project, we should reconsider the balance between the pressure recovery and the shock strength as one critical design feature of this specific airfoil design for HLFC.

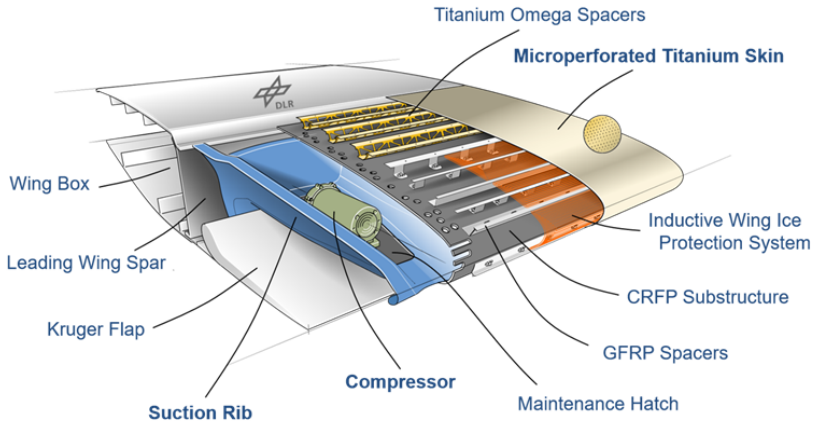

Fig. 8: Proposed structure and system solution for the wing.

The envisaged structure of the HLFC wing is shown in Figure 8. The difference between a wing and a VTP is that the leading edge of a wing is not empty, but houses both high-lift and de-icing system. As usual for a laminar wing, a Krueger system is installed to keep the upper side of the wing undisturbed, thus allowing laminar flow.

Due to the space needed for the Krueger system, the space for the HLFC system is very limited, making a system with small suction chambers discharging the sucked air via throttle holes into a large plenum or duct unfeasible. The solution is to design fewer and larger suction chambers allowing for a simpler structure to support the microperforated sheet. Our solution is based on a microperforated skin with porosity variation in chordwise direction. This would make an HLFC system with only one large suction chamber or plenum possible. The functionality of this one-chamber approach has been validated by DLR in a large scale wind tunnel test [9].

If a laser-drilling process is used to produce the microperforated suction sheet, the easiest method for varying the porosity is to vary the hole pitch. This allows the manufacturer to keep the settings of the laser constant, so that all suction holes have approximately the same geometry. Based on samples, which were tested with the laminar flow meter [10], twenty possible microperforations were defined together with the manufacturer. Considering these manufacturable microperforations, we propose a design[2] with five regions and the four different microperforations presented in Table 3. Their pressure-loss characteristics are presented in Figure 9a, which also shows the pressure-loss charcteristic used for the A320 HLFC VTP. We see that the A320 characteristics is comparable to the most open microperforation with pitch 500 μm.

[2] Another design based on ten regions and nine different microperforations can be found in [1].

Pitch	[μm]	500	800	900	1100
A	[Pa m/s]	9990	25574	32367	48351
B	[Pa m/s^2]	25606	167814	268805	599845

Table 3: Manufacturable microperforations used for the design. Pitch in μm.

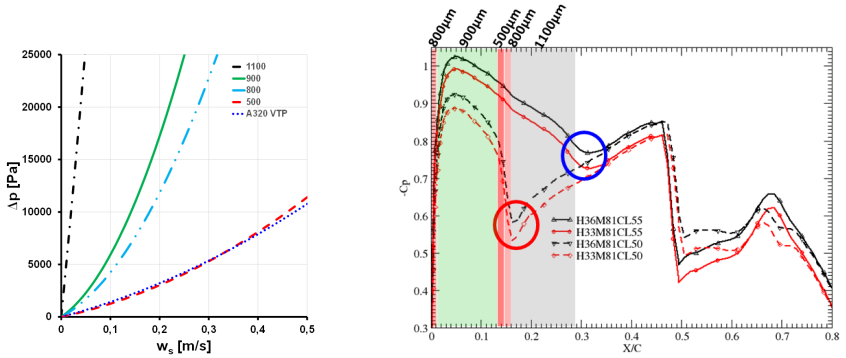

(a) Pressure-loss characteristics. (b) C_p-distributions and microperforations.

Fig. 9: Five regions with four different microperforations.

The regions in which the different microperforations are used, are indicated with different colors in Figure 9b. We notice a short region with pitch 800 μm near the stagnation point. For the three-dimensional wing, this short region translates into a long and narrow strip with pitch 800 μm along the leading edge. Furthermore, there are two additional short regions with pitch 500 μm and 800 μm where the boundary layer is close to separation, indicated by the red circle. Here we need some extra suction as previously mentioned.
In Figure 10 we present the Reynolds number Re_{δ_1} and the form factor H_{12} for 33000 ft, Mach = 0.81, $C_L = 0.50$, i.e. in the case of Figure 7 obtained with the boundary layer code COCO [11]. We observe the rapid increase in H_{12} at $X/C = 0.14$, which is limited by strong suction. Without applying suction that is strong enough, the laminar boundary layer would separate at this location.
In Figure 9b we also show the C_p-distribution with the longest pressure-recovery zone, which, in this case, extends beyond the end of the suction panel marked by the blue circle.
In Figure 11 we present some N-factor results obtained with the stability code LILO [12]. We see that the Tollmien-Schlichting N-factors are very small. If no problem with separation arises, we could reduce the suction without causing early TS-transition.

5 Conclusions

In this paper, we compared the A320 HLFC VTP design with the design of an HLFC system for the wing of a long-range transport aircraft in the context of

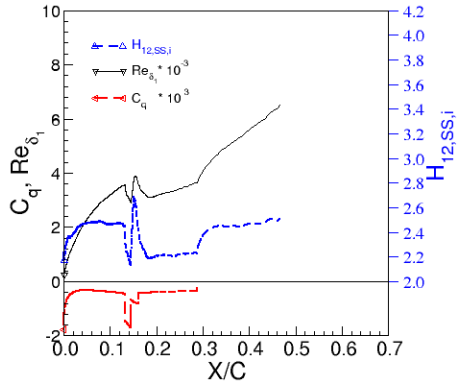

Fig. 10: Re_{δ_1} and H_{12} for the case of Figure 7.

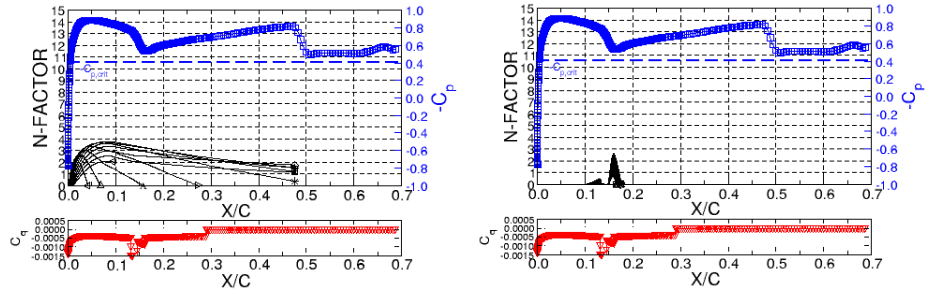

(a) Crossflow N-factors. (b) Tollmien-Schlichting N-factors.

Fig. 11: N-factor results for the case of Figure 7.

the HLFC-WIN project. In the first design, we used one microperforation and adjusted the suction strength with the help of suction chambers. In the second design, we applied the concept of variable microperforation and showed that this concept is feasible. This concept definitely deserves more attention. Future work should address the following points:

1. Reconsideration of the balance between pressure recovery and the shock strength.
2. Replacement of each pressure-loss characteristic by a range of allowable ones to allow for inaccuracies in the laser-drilling process.
3. Inclusion of no-suction zones caused by the supporting structure in the design calculations.

Acknowledgments and disclaimer

The authors thank Martin Radestock for his support and Nancy Schrauf for editing.

The A320 flight test activities received funding from the European Community's Seventh Framework Programme FP7/2007-2013, under grant agreement no 604013, AFLoNext project.
The HLFC-WIN project received funding from the Clean Sky 2 Joint Undertaking (JU) under grant agreement CS2-LPA-GAM-2020-2023-01. The JU receives support from the European Union's Horizon 2020 research and innovation programme and Clean Sky 2 JU members not in the Union.

The results, opinions, conclusions, etc. presented in this work are those of the authors only and do not necessarily represent the position of the JU; the JU is not responsible for any use made of the information contained herein.

References

1. Streit, T., Kruse, M., Kilian, T., von Geyr, J., Petropoulos, I., "Aerodynamic Design and Analysis of HLFC Wings within the European Project HLFC-WIN." 33rd Congress of the International Council of the Aeronautical Sciences (ICAS), Stockholm, Sweden, 4-9 September 2022.
2. Schrauf, G., von Geyr, H., "Hybrid Laminar Flow Control on A320 Fin: Retrofit Design and Sample Results." AIAA Journal of Aircraft (2021), Vol. 58, No. 6, November-December 2021, pp. 1272-1280. https://arc.aiaa.org/doi/10.2514/1.C036179.
3. Schrauf, G., von Geyr, H., "Simplified Hybrid Laminar Flow Control for the A320 Fin - Part 2: Evaluation with the e^N-method." AIAA SciTech Forum, 11-15 & 19-21 January 2021, Virtual Event. AIAA Paper AIAA-2021-1305. https://arc.aiaa.org/doi/10.2514/6.2021-1305.
4. Schrauf, G., "Large-Scale Laminar-Flow Tests Evaluated with Linear Stability Theory." AIAA Journal of Aircraft, Vol. 41, No. 2, March-April 2004, pp. 224 - 230. https://arc.aiaa.org/doi/10.2514/1.C036179.
5. Arnal, D., Juilien, J. C., Reneaux, J., Gasparian, G., "Effect of Wall Suction on Leading-Edge Contamination." Aerospace Science and Technology, No. 8 (1997), pp. 505-571.
6. Methel, J., Méry, F., Forte, M., Vermeersch, O., "Laminar Flow Control along the Attachment Line of a Swept Wing." ECCOMAS 2022, Oslo, Norway.
7. MacManus, D.G., Eaton, J.A., "Flow physics of discrete boundary layer suction - measurements and predictions." J. Fluid Mech. (2000), vol. 417, pp. 47-75.
8. Schrauf. G., "On allowable surface tolerances for laminar flow." DLR-IB-AS-BS-2022-70, June 2022, https://elib.dlr.de/187060/.
9. Kilian, T., Horn, M., "Verification of a chamberless HLFC design with an outer skin of variable porosity." CEAS Aeronautical Journal 12 (2021), pp. 835–845 (2021). https://doi.org/10.1007/s13272-021-00528-4.
10. Seitz, A., "Messkörper, Durchflussmesssystem und Computerprogramm dafür," Offenlegungsschrift DE 2015 113 999 A1 2016.03.03, Anmeldetag 24.08.2015, Offenlegungstag 03.03.2016, Deutsches Patent- und Markenamt.
11. "COCO - A Program to Compute Velocity and Temperature Profiles for Local and Nonlocal Stability Analysis of Compressible, Conical Boundary Layers with Suction," *ZARM Technik Report*, November 1998.
12. Schrauf, G., "LILO 2.1 User's Guide and Tutorial," Bremen, Germany, *GSSC Technical Report* No. 6, originally issued 2004, modified for Version 2.1 July 2006.